Third International Conference on Sustainable Construction Materials and Technologies http://www.claisse.info/Proceedings.htm

Cracking sensibility of slag cement concrete at early age

A. Darquennes and F. Benboudjema

ENS Cachan CNRS UMR8535/UPMC/PRES Université Sud Paris, Cachan, France
aveline.darquennes@ens-cachan.fr, farid.benboudjema@ens-cachan.fr

ABSTRACT

Slag cement concrete is widely used on all kinds of civil engineering structures because of its advantages comparing to Portland cement concrete (eg. lower hydration heat, lower permeability). The production of this cement is also more respectful to the environment, since slag is a waste industrial byproduct of steel production. Nevertheless, the use of slag cement concrete can lead to an increase of cracking sensitivity at early age under restrained deformations. Based on the results of a large experimental campaign, this article presents the first simulations on the behaviour of a civil engineering structure made with this type of concrete considering three different slag contents (0, 42 and 71%). It is shown that the crack sensitivity is larger than that of a Portland cement concrete, especially for larger slag contents. This is due to its slower hydration kinetics which delays the development of tensile strength and the faster evolution rate of its autogenous shrinkage and Young modulus.

Keywords. Blast-furnace slag, Cracking, Creep, Mineral additions, Shrinkage.

INTRODUCTION

Nowadays, the blast-furnace slag, a by-product of the steel industry, is often used as aggregate or/and mineral addition characterized by latent hydraulic properties to produce cementitious materials. Part of the clinker being replaced by slag, the CO_2 emissions of the cement industry are found reduced (De Larrard, 2009). This is the reason why slag cement is generally considered as an eco-material. Moreover, it is characterized by a low permeability and a good sulphate resistance (Bijen, 1998). Thanks to these advantages, various civil engineering structures, such as roads, bridges and tanks, have been realized with slag cement concretes.

Nevertheless, some of these structures showed cracking at early age due to the restriction of their deformations. Indeed, massive structures are submitted to several types of deformations related to cement hydration. Due to the water consumption by cement, capillary depressions appear inside the cementitious matrix leading to a global contraction of the material (autogenous shrinkage). The chemical reaction being exothermal, a thermal dilation followed by contraction characterizes the behaviour at early age (thermal shrinkage). When the volume deformations are restrained, for example by existing structures (e.g. slab), tensile stresses appear leading to cracking.

A previous experimental campaign (autogenous shrinkage, heat release, etc) realized on concrete samples with different slag contents (Darquennes et al, 2011) showed that the studied slag cement concretes are characterized by faster kinetics and larger amplitudes of free autogenous deformation. Due to their significant compressive creep, they also have a greater capacity to relax internal stresses. This article presents the first simulations on the behaviour of a civil engineering structure made with this type of concrete considering three different slag contents (0, 42 and 71%). The objective is to study the cracking sensitivity at early age under restrained conditions.

MATERIAL CHARACTERISTICS

The behaviour of three cements is studied hereafter: a Portland cement CEM I 52.5 N and two blended cements, namely CEM III/A 42.5 LA and CEM III/B 42.5 HSR LA. Their slag content is different while their clinker and slag are of the same origin. The blended cements (CEM III/A and CEM III/B) contain 42% and 71% of slag respectively and have similar specific areas and densities. The respective concretes are indicated in this paper as CEM I, CEM III/A and CEM III/B. Their water-binder ratio (w/b) and the binder (clinker + slag) content are kept identical and equal to 0.45 and 375 kg/m³ respectively. Six different fractions of aggregates are used. Details of the concrete mixture proportions are given in Table 1.

Table 1. Concrete Mixture Compositions (kg/m^3)

	CEM I	CEM III/A	CEM III/B
Cement	375	375	375
Water	164.6	166.95	164.9
Admixture	5.63	2.63	5.25
Sand 0/0.5	492	492	492
Sand 0.5/1	126	126	126
Sand 1/3	104	104	104
Limestone gravel 2/6	311	311	311
Limestone gravel 6/10	438	438	438
Limestone gravel 10/14	415	415	415

CONSTITUTIVE MODEL

At early age, the behaviour of the concrete mixtures (mechanical properties, autogenous deformation) depends strongly on the kinetics of the cement hydration, described often by an intrinsic parameter named “hydration degree”. The hydration degree ξ is defined as the ratio between the hydrated cement content at a time t and the initial anhydrous cement content. In this study, the evolution of hydration is controlled by the use of the chemical affinity function $\tilde{A}(\xi)$ (Eq.1, Ulm and Coussy, 1998). This parameter is determined experimentally from adiabatic calorimetry tests (Darquennes et al, 2013). A polynomial fit of the chemical affinity is used in the model implemented into the finite element code Cast3M (developed by the French Atomic Energy Commission). This relation gives the best agreement with the experimental data. The activation energy E_a is determined from mechanical tests realized on concrete samples kept at 10°C and 30°C (Darquennes et al, 2010). The value of this parameter increases with the slag content and it is found equal to 27, 43 and 48 kJ/mol for the CEM I, CEM III/A and CEM III/B respectively.

$$\dot{\xi}=\tilde{A}(\xi)\, e^{-E_a/RT} \quad (1)$$

Where R is the ideal gas constant 8.3145 [J.K^{-1}mol^{-1}] and T is the temperature [K].

The energy balance equation (Eq.2), which includes the heat release due to the hydration reaction, is solved to obtain the temperature evolution. In this study, the thermal properties (thermal conductivity k, latent hydration heat L, volumetric heat capacity C, dilation coefficient α and activation energy E_a) are kept constant. Indeed, previous numerical simulations (Briffaut et al, 2012) showed that the temperature field is not significantly affected by the variation of these parameters. From the temperature evolution, the thermal deformations are determined (Eq.3).

$$C\ \frac{\partial T}{\partial t} = \nabla(k\nabla T) + \ L\,\dot{\xi} \quad (2)$$

$$\dot{\varepsilon}^{th} = \ \alpha\,\dot{T} \quad (3)$$

The autogenous deformation is often described using a linear relation depending on the hydration degree. However, this approach is not able to take into account the expansion measured at early age for slag cement concretes (Darquennes et al, 2010). In this work, a non-linear relation is proposed to fit the autogenous deformation depending on several parameters as the value of the maximal swelling deformation, the correspondent hydration degree and the final value of shrinkage. Notice that the effect of drying shrinkage on the cracking sensibility of the studied structure was not taken into account because this phenomenon evolves slowly and its effect is negligible at early age. In order to predict the evolution of the mechanical properties (Young modulus, tensile and compressive strength), relations based on the advancement of the hydration reaction (De Schutter et al, 1996) are also adopted (Eq. 1 and 4).

$$X(\xi) = X_\infty \left(\frac{\xi(t)-\xi_0}{\xi_\infty-\xi_0}\right)^{a_x} \quad (4)$$

Where X_∞ is the final value of the parameter (i.e. when $\xi_=\xi_\infty$), ξ_0 is the percolation threshold (equal to 0.14, 0.16 and 0.20 for CEM I, CEM III/A and CEM III/B respectively) and the coefficients a_x are determined from the experimental data (Darquennes et al, 2011).

The basic creep is described with one aging Kelvin-Voigt unit and one dashpot placed in serial. The corresponding differential equation, the stiffness parameter and the dashpot viscosities follow Equations 5, 6 and 7 respectively. The parameters of the Kelvin-Voigt unit are determined from experimental compressive creep tests (Darquennes et al, 2011).

$$\tau_{bc}\ddot{\varepsilon}^1_{bc} + \left(\tau_{bc}\frac{\dot{k}_{bc}(\xi)}{k_{bc}(\xi)} + 1\right)\dot{\varepsilon}^1_{bc} = \frac{\ddot{\tilde{\sigma}}}{k_{bc}(\xi)} \text{ and } \tilde{\sigma} = \eta^2_{bc}(\xi)\dot{\varepsilon}^2_{bc} \quad (5)$$

$$k_{bc}(\xi) = k_{bc\_\infty}\frac{0.473}{2.081-1.608\bar{\xi}}\bar{\xi}^{a_x} \quad (6)$$

$$\eta_{bc}^2(\xi) = \eta_{bc\_\infty}^2 \frac{0.473}{2.081 - 1.608\bar{\xi}} \bar{\xi}^{a_x} \tag{7}$$

Where τ_{bc} is the characteristic time (constant), $k_{bc}(\xi)$ is the spring stiffness (increasing with the hydration degree), $\tilde{\sigma}$ is the effective stress, η_{bc}^2 is the apparent viscosity of the dashpot placed in serial and k_{bc_∞} is the final stiffness.

The mechanical behaviour of concrete is modelled by an elastic-damage model coupled with creep, which takes into account the evolution of the elastic stiffness with the hydration degree (De Schutter et al, 1996) and with damage (Mazars, 1986). The relationship between apparent stresses $\boldsymbol{\sigma}$, effective stresses $\tilde{\boldsymbol{\sigma}}$, damage *D*, elastic stiffness tensor **E**, elastic strains $\boldsymbol{\varepsilon}_{el}$, basic creep strains $\boldsymbol{\varepsilon}_{bc}$ and total strains $\boldsymbol{\varepsilon}$ reads:

$$\boldsymbol{\sigma} = (1-D)\tilde{\boldsymbol{\sigma}} \text{ and } \dot{\tilde{\boldsymbol{\sigma}}} = \mathbf{E}(\xi)\dot{\boldsymbol{\varepsilon}}_{el} = \mathbf{E}(\xi)\left(\dot{\boldsymbol{\varepsilon}} - \dot{\boldsymbol{\varepsilon}}_{bc} - \dot{\boldsymbol{\varepsilon}}_{au} - \dot{\boldsymbol{\varepsilon}}_{th}\right) \tag{8}$$

D is linked to the elastic equivalent tensile strain $\hat{\varepsilon}$ and is coupled with creep using a constant coefficient β:

$$\hat{\varepsilon} = \sqrt{\left\langle \boldsymbol{\varepsilon}_{el} + \beta\boldsymbol{\varepsilon}_{bc} \right\rangle_+ : \left\langle \boldsymbol{\varepsilon}_{el} + \beta\boldsymbol{\varepsilon}_{bc} \right\rangle_+} \tag{9}$$

The damage evolution reads:

$\dot{D} = 0$ if $\hat{\varepsilon} \le \kappa_0(\xi)$

And the evolution of damage is given by

$$D = 1 - \frac{\kappa_0}{\hat{\varepsilon}}\left[(1+A_t)\exp(-B_t\hat{\varepsilon}) - A_t\exp(-2B_t\hat{\varepsilon})\right] \text{ if } \hat{\varepsilon} \ge \kappa_0(\xi) \tag{10}$$

where $\kappa_0(\xi)$ is the tensile strain threshold, A_t and B_t are constant material parameters controlling the softening branch in the stress-strain curve (tension).

The evolution of the tensile strain threshold depends on the Young modulus (Eq. 4) and the tensile strength (Eq. 11). Notice that size effect on the tensile strength is taken into account thanks to a reduction coefficient equal to 0,77 (Van Vliet and van Mier, 1999).

$$\kappa_0(\xi) = \frac{f_t(\xi)}{E(\xi)} = \frac{f_{t\infty}}{E_\infty}\bar{\xi}^{\gamma-\beta} \tag{11}$$

All these relations were implemented into the Cast3M finite element code.

NUMERICAL SIMULATION

We analyse hereafter the evolution of temperature, stresses and damage in a wastewater treatment plant (Figure 1). The finite element mesh represents a wall that has just being cast on a slab. Axisymmetric conditions are imposed and the reinforcement is not taken into account. The formwork is taken off at 1 day. Initial and ambient temperatures are considered equal to 25°C and 20°C respectively. The thermal exchange coefficients are equal to 10, 0.8 and 0.6 W/m²K for the natural conditions, formwork and ground respectively (Clément, 2004). The boundary conditions are assumed of convective type.

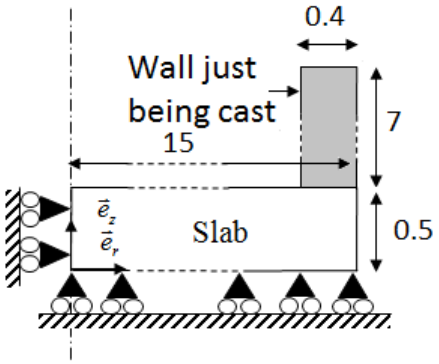

Figure 1. Wastewater treatment plant (dimensions in m)

Temperature evolution. Figure 2 represents the evolution of the temperature for the three studied concretes at the core and near the surface of the wall. The temperature evolves faster for CEM I. Maximum values are found equal to 63°C, 58°C and 53°C for CEM I, CEM III/A and CEM III/B respectively. After the formwork removal, the temperature in the wall decreases and the thermal gradient between the wall core and its skin increases significantly. After 3 days, the temperature of the wall is equal to the ambient temperature for all the studied concretes.

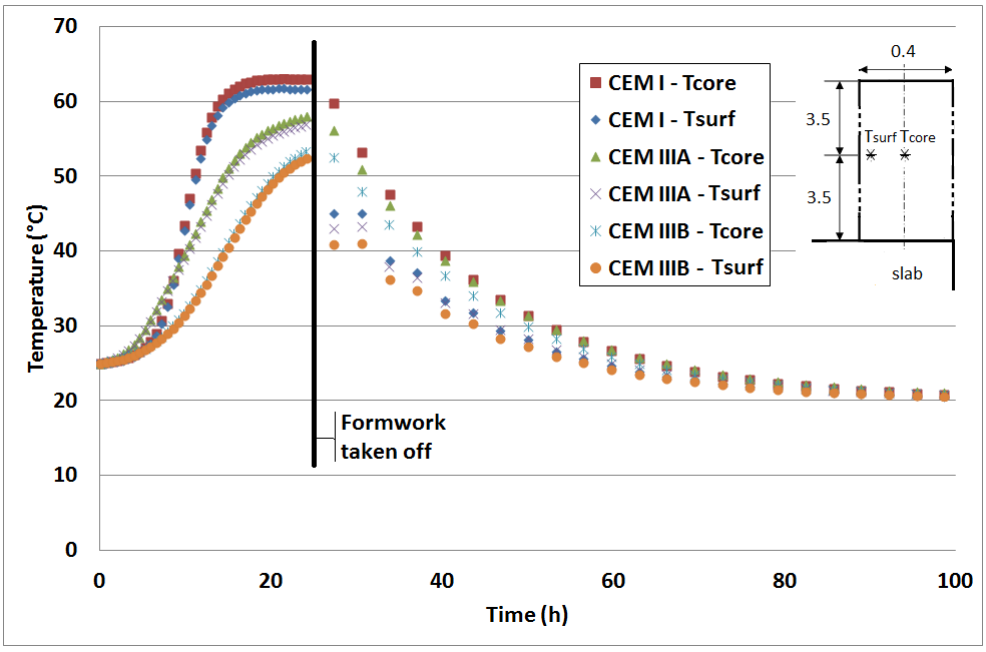

Figure 2. Temperature evolution in the centre (T_{core}) and near the surface of the wall (T_{surf})

Stresses and damage evolution. Figures 3 and 4 show the evolution of the vertical and orthoradial stresses at two positions (named #1 and #2) close to the slab. This area is very sensitive due to the restriction of the wall deformation by the slab. Indeed, the damage appears first in this part of the wall at about 10 hours after the mixing and this for all the studied concretes. Tensile stresses appear in position #1 and compressive stresses in position #2. At early age, these stresses increase rapidly due to the restriction of the thermal

expansion for CEM I and CEM III/A. This effect is found more pronounced for CEM I, which agrees with its thermal evolution (Fig.2). The autogenous deformation of CEM III/B seems the major parameter affecting the stresses evolution at very early age. After the formwork removal, the sign of the compressive and tensile stresses alternates and their (absolute) values increase significantly for all the studied concretes. Notice that CEM III/B is characterized by important tensile stresses (P2) close to the tensile strength of a healthy material (Fig.5) despite its larger capacity to relax stresses (see its large compressive creep). Nevertheless, these stresses are found smaller to the stresses obtained from an elastic computation.

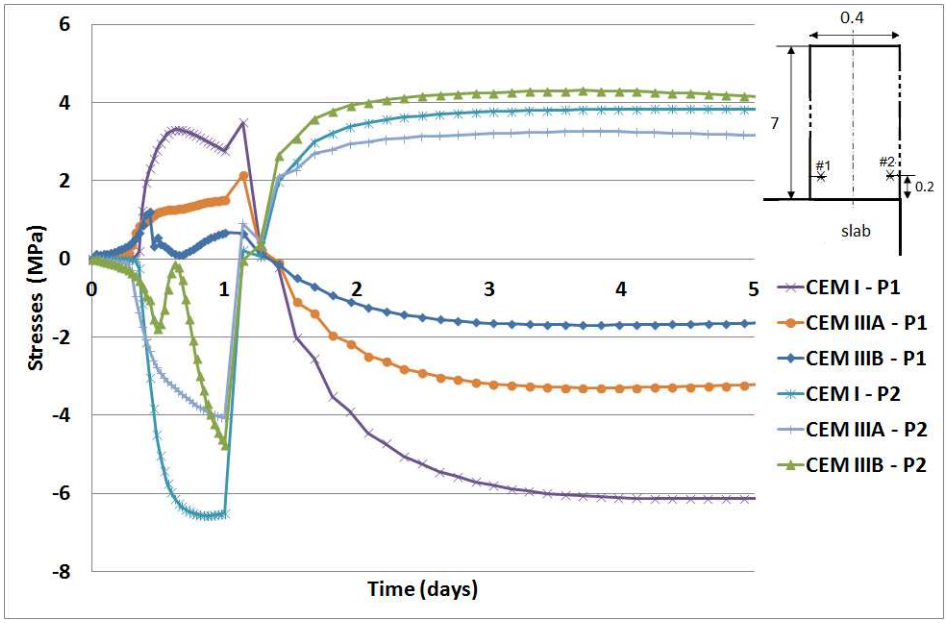

Figure 3. Evolution of vertical stresses

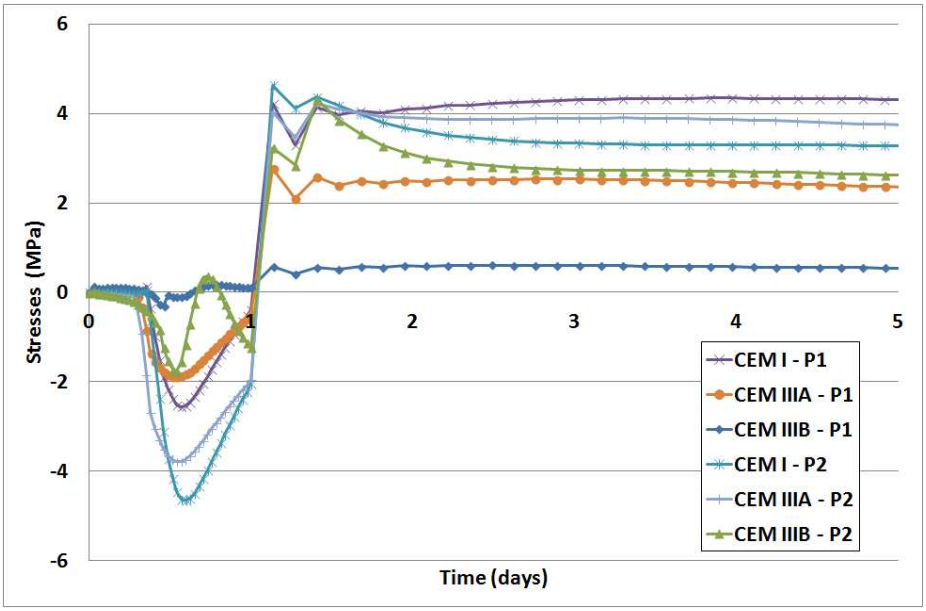

Figure 4. Evolution of orthoradial stresses

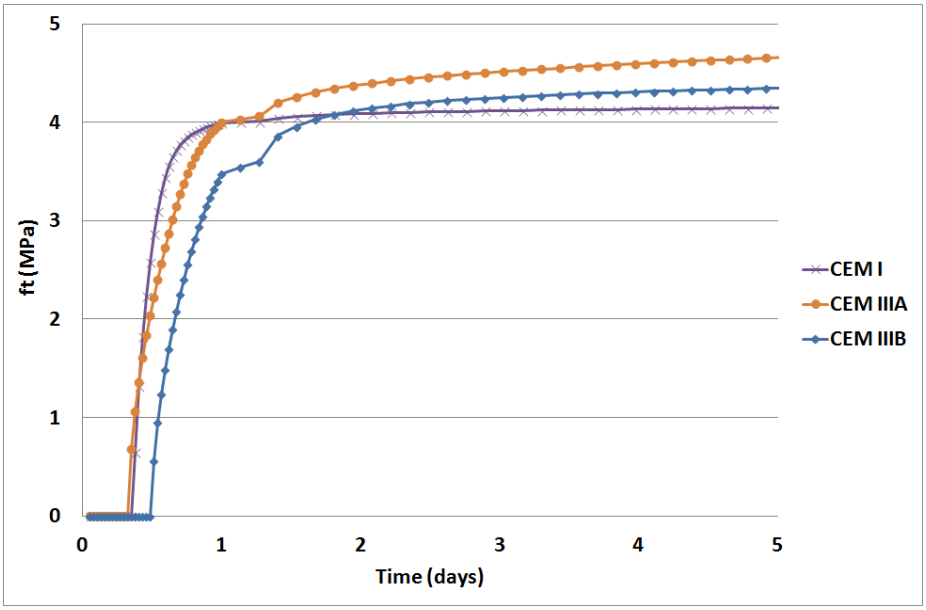

Figure 5. Evolution of tensile strength based on the equation 4

Figure 6 shows the evolution of damage D at the two positions (#1 and #2) close to the slab. The value of D evolves from 0 (healthy material) to 1 (completely damaged material). The analysis of the damage pattern (Fig.7) shows clearly that cracking appears at the binding between the wall and the slab for all the studied concrete mixtures. The wall cast with the CEM III/B mixture is found more damaged and it is also characterized by an important value of D at early age at #1 (Fig.6). This observation is also confirmed by looking at the evolution of stresses at #1 (Fig.3 and 4). The lower part of the wall is more damaged for CEM I than for CEM III/A. This difference of behaviour is due to the thermal gradient which is more important for CEM I (Fig.2).

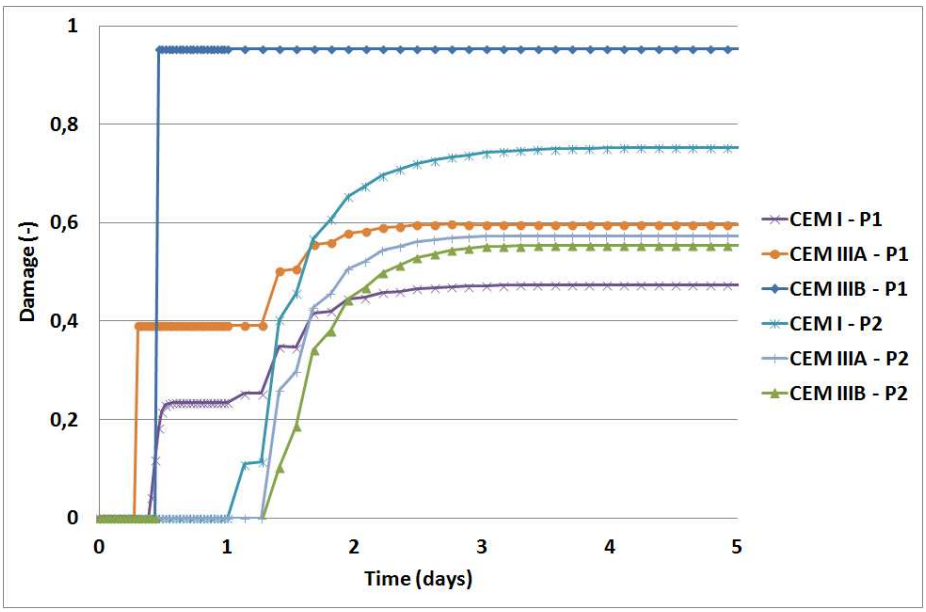

Figure 6. Evolution of damage at early age

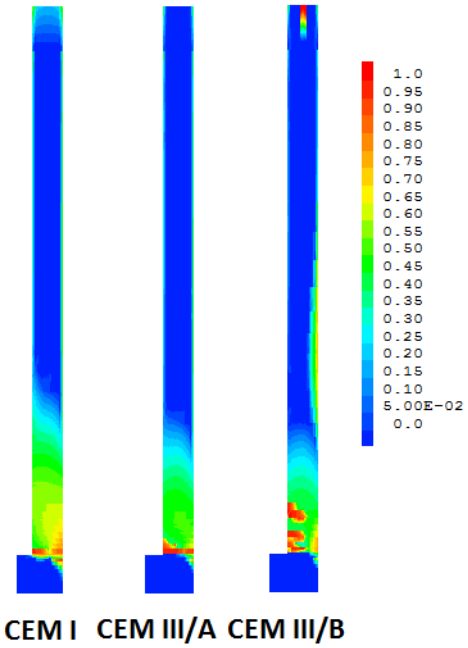

Figure 7. Damage pattern in the wall and the slab after 28 days for the three studied compositions

CONCLUSIONS

These first simulations of the behaviour of a waterwaste treatment tank made considering various slag contents (0, 42 and 71%) confirm the sensitivity (larger damage) to cracking at early age for the slag cement concretes with significant slag content. This behaviour is probably related to their slower hydration kinetics delaying the tensile stresses evolution and the faster evolution rate of their shrinkage and Young modulus. The results also underline the significant effect on the stresses evolution of the time when the formwork is taken off. Further studies are necessary to confirm and generalise these observations considering the influence of the variability of the parameters characterizing the material behaviour (apparent activation energy, latent hydration heat, volumetric heat capacity, strength, Young modulus etc.) and the type and the duration of curing.

REFERENCES

Bijen, J. (1998). “Blast furnace slag cement for durable marine structures”, CIP Royal Library Den Haag, Stichting Betonprisma,‘s-Hertogenbosch, The Netherlands.

Briffaut, M., Benboudjema, F., Torrenti, J.-M., and Nahas, G (2011). “Numerical analysis of the thermal active restrained shrinkage ring test to study the early age behavior of massive concrete structures”, *Engineering Structures*, 33 :1390-1401.

Briffaut, M., Benboudjema, F., Torrenti, J.-M. and Nahas, G. (2012). “Early age behaviour of a massive concrete structure: Effects of thermal boundary conditions and thermal

properties evolutions on temperature and stress fields", *European Journal of Environmental and Civil Engineering*, 16:589-605.

Clement, J.L. (2004). "Exemple de calcul en Europe", *Comportement du béton au jeune âge* (Traité MIM, série Matériaux de construction), ACKER Paul, TORRENTI Jean-Michel, ULM Franz-Josef.

Darquennes, A., Staquet, S., Kamen, A., Delplancke-Ogletree, M.-P. and Espion B. (2009). "Early age properties development of concrete with different slag contents", *ACI SP-259, Transition from Fluid to Solid : Re-examining the Behavior of Concrete at Early Ages*, San Antonio, Texas, USA, 43-66.

Darquennes, A., Staquet, S., Delplancke-Ogletree, M.-P. and Espion, B. (2011). "Effect of autogenous deformation on the cracking risk of slag cement concretes", *Cement and Concrete Composites*, 33: 368-379.

Darquennes, A., Staquet, S. and Espion, B. (2011). "Determination of time-zero and its effect on autogenous deformation evolution", *EJECE*, 15: 787-798.

Darquennes, A., Staquet, S. and Espion, B. (2011). "Behaviour of slag cement concrete under restraint conditions", *EJECE*, 15: 1017-1029.

Darquennes, A., Staquet, S. and Espion, B. (2013). "How to assess the hydration of slag cement concretes?", *Construction and Building Materials*, http://dx.doi.org/10.1016/j.conbuildmat.2012.09.087

De Larrard, F. (2009). "Quelques questions soulevées par analyses du cycle de vie des infrastructures routières", *Bulletin du Laboratoire des Ponts et Chaussées*, 276 : 1-8.

De Schutter, G. and Taerwe, L., (1996). "Degree of hydration based description of mechanical properties of early-age concrete", *Materials and Structure*, 29 :335-344.

Mazars, J., (1986) "A description of micro and macroscale damage of concrete structures", *Engineering Fracture Mechanics*, 25 : 143-150.

TC107-CSP (1998). "Measurement of time-dependent strains of concrete", *Materials and Structures*, 31: 507-512.

Ulm F-J., and Coussy O., (1998). "Couplings in early-age concrete: From material modeling to structural design", *International Journal of Solids and Structures*, 35 (31-32): 4295-4311.

Van Vliet, M. R.A. and Van Mier, J. G.M., (1999), "Effect of strain gradients on the size effect of concrete in uniaxial tension", *International Journal of Fracture*, 95: 195–219.